Advanced Ceramics Progress: Vol. 11, No. 4, (Autumn 2025) 55-61

Materials and Energy Research Center
MERC

Contents lists available at ACERP

Advanced Ceramics Progress

Journal Homepage: www.acerp.ir

Original Research Article

Investigation of Fused Filament Fabrication Parameters for Producing Mechanically Stable SiC/Polymer Composite Green Parts

Mohammad Solgi[a], Raziyeh Ghelich [b], Hamid Omidvar [c,d*]

[a] MSc Student, Department of Materials and Metallurgical Engineering, Amirkabir University of Technology, Tehran, 1599637111, Iran.
[b] Ph.D., Department of Nanotechnology and Advanced Materials, Materials and Energy Research Center, Karaj, P.O. Box 31787-316, Iran.
[c] Associate Professor, Department of Materials and Metallurgical Engineering, Amirkabir University of Technology, Tehran, 1599637111, Iran.
[d] Associate Professor, Center for International Scientific Studies and Collaborations (CISSC) of Iran, Tehran, Iran.

* Corresponding Author Email: Omidvar@aut.ac.ir (Hamid Omidvar) URL: https://www.acerp.ir/article_252664.html

ARTICLE INFO

Article History:

Received 17 July 2026
Revised 12 August 2026
Accepted 03 September 2026

Keywords:

Fused Filament Fabrication (FFF),
Printing Parameters,
SiC Filament,
Additive Manufacturing,
Green Parts

ABSTRACT

Silicon carbide (SiC) is a non-oxide technical ceramic with outstanding mechanical, thermal, and chemical properties; however, its high hardness and brittleness limit the fabrication of complex geometries using conventional manufacturing routes. Fused filament fabrication (FFF) provides a cost-effective approach for shaping ceramic-polymer composites, although obtaining high-quality green parts remains challenging due to the sensitivity of ceramic-filled filaments to printing conditions. In this study, the printability of a commercial PE/α-SiC composite filament containing 52 vol.% SiC was investigated through thermal, microstructural, and mechanical evaluations. Thermal analysis was performed to evaluate the thermal behavior and decomposition characteristics of the composite filament, while the microstructure and mechanical performance of the fabricated green parts were evaluated under selected printing conditions. Thermal analysis revealed relatively limited mass loss below approximately 360 °C and a major binder degradation region between 360 and 474 °C. The selected printing conditions, including a layer height of 0.4 mm, 100% linear infill density, one shell, nozzle temperature of 250 °C, bed temperature of 60 °C, printing speed of 15 mm s^{-1}, and flow rate of 110%, enabled the fabrication of mechanically stable green parts. SEM observations revealed improved filament contact and fewer visible inter-bead gaps compared with the comparative printed specimen. The fabricated green parts exhibited an average flexural strength of 10.5 ± 2.5 MPa, indicating adequate mechanical integrity in the as-printed state. Furthermore, the successful fabrication of a complex-shaped green component demonstrated the capability of the selected FFF processing conditions to produce geometrically complex SiC/polymer green parts using a commercial composite filament. The present study provides a baseline for subsequent investigations of the debinding and sintering of FFF-printed SiC components.

https://doi.org/10.30501/acp.2026.592047.1203

1. INTRODUCTION

Silicon carbide (SiC) is one of the most important non-oxide technical ceramics due to its outstanding combination of high hardness, wear resistance, chemical stability, thermal conductivity, and excellent stability at elevated temperatures. These unique properties have enabled its application in demanding fields, including

Please cite this article as: Solgi, M., Ghelich, R., & Omidvar, H. (2025). Investigation of Fused Filament Fabrication Parameters for Producing Mechanically Stable SiC/Polymer Composite Green Parts. *Advanced Ceramics Progress*, *11*(4), 55-61. https://doi.org/10.30501/acp.2026.592047.1203

high-temperature components, wear-resistant systems, electronic devices, and energy-related technologies. However, the intrinsic brittleness, high hardness, and poor machinability of SiC make the fabrication of complex-shaped components challenging using conventional manufacturing approaches (Deckers et al., 2014; Jose et al., 2026; Mansfield et al., 2019; Travitzky et al., 2014; Zocca et al., 2015). Traditional ceramic shaping techniques, such as pressing, slip casting, and injection molding, are widely used for manufacturing ceramic components; however, these methods often require expensive tooling, complex processing steps, and long production cycles. In addition, the fabrication of customized geometries, internal channels, porous architectures, and low-volume components remains difficult and economically inefficient using conventional routes (Camargo et al., 2022; Fan et al., 2024). These limitations have encouraged the development of advanced manufacturing approaches capable of producing complex ceramic structures with reduced processing constraints (Mansfield et al., 2019).

Additive manufacturing (AM), commonly known as three-dimensional (3D) printing, has emerged as a promising alternative for fabricating ceramic components with complex geometries and reduced material waste. Among various ceramic AM technologies, including stereolithography (SLA), digital light processing (DLP), binder jetting, and material extrusion-based processes, fused filament fabrication (FFF) has attracted increasing attention due to its simplicity, low equipment cost, and accessibility (Abdulhameed et al., 2019; Alfattni, 2022; Jiménez et al., 2019). In FFF, ceramic-filled polymer composite filaments are extruded through a heated nozzle to construct three-dimensional green parts layer by layer. Compared with other ceramic AM techniques, FFF provides a cost-effective route for rapid prototyping and low-volume production while enabling the fabrication of complex structures using commercially available printing platforms (Arnesano et al., 2020; Furong et al., 2022; Orlovská et al., 2020; Zhao et al., 2021).

Despite the advantages of FFF for ceramic shaping, obtaining high-quality green parts remains challenging due to the complex interaction between filament properties and printing conditions. The final structural integrity of printed components is strongly influenced by processing parameters such as extrusion temperature, layer height, deposition strategy, material flow, and printing speed. Improper selection of these parameters may result in incomplete inter-bead fusion, internal void formation, poor interlayer adhesion, and reduced mechanical performance. These challenges become more pronounced for ceramic-filled filaments because of their high ceramic solid loading, which limits melt flow behavior and increases sensitivity to processing conditions, even when the polymer binder fraction is comparatively high (Gómez-Gómez et al., 2021).

Recent studies have demonstrated the feasibility of fabricating silicon carbide components using commercially available SiC/polymer composite filaments through FFF followed by debinding and high-temperature sintering processes (Gauthe et al., 2025; Ghelich et al., 2026; Goulas et al., 2025). These investigations have mainly focused on the influence of thermal treatment conditions, densification behavior, phase evolution, and mechanical properties of the final sintered SiC components. For example, the use of Zetamix SiC/polymer filament has shown the potential of FFF as a viable approach for producing complex SiC components after suitable debinding and sintering treatments. However, the quality of the initial green part produced by FFF remains a critical factor for the success of subsequent ceramic conversion processes (Goulas et al., 2025; Vozarova et al., 2023). Therefore, a detailed understanding of the relationship between printing conditions, defect formation, microstructural characteristics, and mechanical behavior of as-printed SiC/polymer composite parts is still required (Wille et al., 2024).

While previous research has primarily focused on the debinding, sintering, and final properties of FFF-printed SiC components, the influence of printing parameters on the structural integrity and mechanical performance of the initial green parts has received comparatively less attention. Therefore, this study focuses on the selection of suitable FFF processing conditions, particularly nozzle temperature, printing speed, and flow rate, based on preliminary printing trials and the thermal behavior of the PE/α-SiC composite filament. The study evaluates the resulting microstructural integrity and mechanical performance of the as-printed green parts prior to thermal treatment. The specific contribution of this study is to relate the selected FFF processing conditions to the resulting green-part microstructure and flexural performance of a commercially available PE/α-SiC filament prior to thermal treatment. Under the selected printing conditions, the fabricated green parts exhibited an average flexural strength of 10.5 MPa, providing a useful baseline for subsequent debinding and sintering studies of FFF-printed SiC components.

2. MATERIALS AND METHODS

2.1. Materials

A commercially available polyethylene-based silicon carbide composite filament (PE/α-SiC, Zetamix, France) was used as the feedstock material for fused filament fabrication (FFF). The filament contained 52 vol.% α-SiC ceramic particles. The commercial filament was supplied with a diameter of 1.75 mm and was used directly for printing and subsequent characterization.

2.2. FFF printing process

Fabrication of the green parts was performed using a Raise3D Pro2 3D printer equipped with a standard extrusion system. The CAD models were converted into STL format and sliced using Ultimaker Cura software. The selection of FFF printing parameters was based on preliminary screening trials and the thermal behavior of the composite filament. Preliminary screening trials were conducted to identify suitable processing conditions that enabled stable extrusion and layer deposition while minimizing severe nozzle clogging, warping, and visible inter-bead defects. The nozzle temperature was set to 250 °C to facilitate melting and flow of the polymer binder and sufficiently reduce the melt viscosity of the highly ceramic-loaded filament (52 vol.% SiC), while remaining below the main binder decomposition region identified by thermal analysis (~360 °C). A low printing speed of 15 mm s^{-1} was chosen to ensure stable extrusion, prevent nozzle clogging due to the high particle loading, and provide adequate thermal residence time for inter-bead fusion. Furthermore, a flow rate of 110% was applied to compensate for inter-bead volumetric gaps inherent to raster deposition, thereby enhancing material density and the contact area between adjacent roads. A bed temperature of 60 °C and a layer height of 0.4 mm were used in combination with a brim structure to ensure strong bed adhesion and prevent thermal warping. Table 1 summarizes the selected printing parameters used for the fabrication of the SiC/polymer green parts.

TABLE 1. Selected FFF printing parameters used for fabrication of SiC/polymer green parts

Parameter	Selected value
Filament diameter	1.75 mm
Layer height	0.4 mm
Infill density	100%
Infill pattern	Linear
Number of shells	1
Nozzle temperature	250 °C
Build platform temperature	60 °C
Printing speed	15 mm/s
Flow rate	110%
Material consumption	~7 g
Printing time	~36 min

2.3. Characterization

2.3.1.Morphological characterization

The morphology and microstructural features of the commercial PE/α-SiC filament and FFF-printed green parts were investigated using scanning electron microscopy (SEM, TESCAN MIRA3, Czech Republic). Prior to SEM examination, the filament and printed specimens were prepared by mechanical polishing, where required, to obtain suitable cross-sectional surfaces for microstructural observation.

2.3.2. Thermal characterization

The thermal behavior of the commercial PE/α-SiC composite filament was evaluated using simultaneous thermal analysis (STA, NETZSCH STA 449 F3 Jupiter, Germany). Thermal analysis was performed from 25 to 1000 °C at a heating rate of 10 °C min^{-1} under an air atmosphere. The obtained TG/DTA curves were analyzed to determine the thermal stability of the binder system, identify the main decomposition regions, and define suitable processing conditions for FFF printing and potential subsequent debinding processes.

2.3.3. Mechanical characterization

The mechanical properties of the fabricated green parts were evaluated using a universal testing machine (SANTAM, Iran). Three-point bending tests were performed according to ASTM D790 using rectangular specimens fabricated under the selected printing conditions. The tests were conducted at a crosshead speed of 1 mm min^{-1}, and the flexural strength (modulus of rupture, MOR) was calculated based on the maximum load recorded at fracture.

The obtained mechanical response was used to evaluate the influence of the FFF processing conditions on the structural integrity of the printed green parts, with particular emphasis on the effects of inter-bead bonding quality and printing-induced defects on the load-bearing capability of the fabricated components.

3. RESULTS AND DISCUSSION

3.1. Thermal analysis of the commercial SiC/polymer composite filament

The thermal behavior of the commercial PE/α-SiC composite filament was investigated by simultaneous thermal analysis (STA) to identify a suitable processing window for the FFF printing process (Figure 1). The filament consisted of 52 vol.% α-SiC ceramic particles and 48 vol.% polymer-based binder, where the thermal response of the polymer phase plays a critical role in determining extrusion behavior and interlayer bonding quality. The TGA curve demonstrates three distinct thermal regions. Up to approximately 360 °C, the filament exhibits high thermal stability with only a minor weight variation, which can be attributed to the removal of absorbed moisture and low-molecular-weight volatile species. This behavior indicates that the composite filament can be processed within the temperature range employed for FFF without significant thermal degradation of the binder (Ghelich et al., 2026). A pronounced weight loss occurs between 360 and 474 °C, corresponding to the main degradation stage of the polymer binder. Approximately 38% of the total mass loss takes place within this temperature interval, indicating the decomposition of the polymeric components. Since this degradation region is considerably higher than the printing temperature, thermal decomposition of the binder during extrusion can be avoided under appropriate processing conditions (Goulas et al., 2025). Based on the obtained thermal characteristics, the selected FFF processing temperature was below the main decomposition region of the PE/SiC composite filament, providing a suitable thermal condition for extrusion without significant binder degradation.

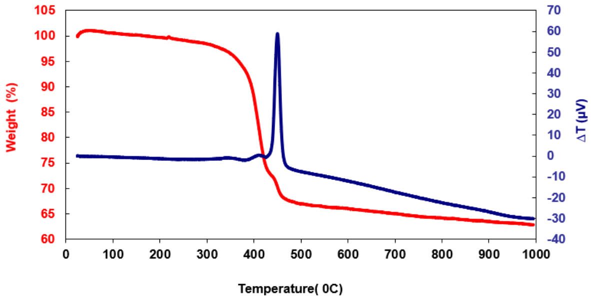

Figure 1. TG/DTA analysis of the filament.

3.2. Microstructural characterization of the commercial SiC/polymer filament

The internal morphology of the commercial PE/α-SiC composite filament was investigated using scanning electron microscopy (SEM). Representative SEM micrographs of the filament cross-section are presented in Figure 2. The micrographs reveal the distribution of α-SiC particles within the polymer-rich matrix. The ceramic particles appear to be relatively uniformly distributed throughout the examined regions, and no obvious large-scale particle agglomeration was observed. The SEM observations were performed to evaluate the distribution of α-SiC particles within the polymer matrix, the quality of inter-bead bonding, and the presence of internal defects, such as voids and microstructural discontinuities, in the filament (Arnesano et al., 2020; Orlovská et al., 2020)

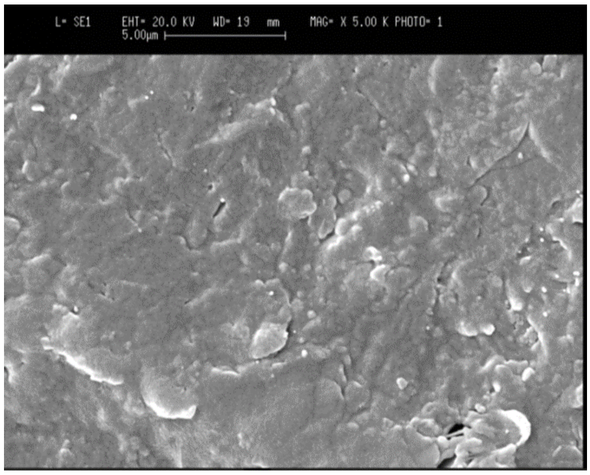

Figure 2. SEM micrographs of the vertical cross-section of the commercial PE/α-SiC composite filament.

3.3. Microstructural evaluation of printed SiC/polymer green parts under selected processing conditions

To compare the internal structure of SiC/polymer green parts fabricated under two selected printing conditions, SEM analysis was performed on representative cross-sections of the printed specimens. Two specimens were selected for comparison: PP1, fabricated under the selected printing condition, and PP2, fabricated under a comparative printing condition.

The selected printing condition used for PP1 consisted of a layer height of 0.4 mm, 100% linear infill density, one shell, nozzle temperature of 250 °C, bed temperature of 60 °C, printing speed of 15 mm s^{-1}, and flow rate of 110%. PP2 was fabricated using a higher printing speed and lower nozzle temperature (layer height: 0.4 mm, 100% linear infill density, nozzle temperature: 200 °C, bed temperature: 60 °C, and printing speed: 35 mm s^{-1}). The comparison between these two conditions was performed to evaluate the effect of printing parameters on filament deposition quality and inter-bead bonding.

The SEM micrographs of PP1 reveal a relatively continuous layered structure with improved contact between adjacent deposited roads. The interfaces between neighboring filaments appear more compact, with fewer visible gaps compared with PP2. In contrast, PP2 exhibits more pronounced discontinuities between deposited roads, including larger inter-bead voids and locally insufficient contact regions. These differences indicate that the selected printing condition promoted improved deposition continuity during the FFF process.

The cross-sectional observations also show the typical layered architecture produced by the FFF process, where individual deposited filaments can be distinguished within the polymer-rich matrix. The SiC particles remain uniformly distributed within the polymer binder after printing, and no obvious particle accumulation or large-scale segregation was observed. These observations suggest that the printing process did not cause obvious large-scale segregation of the ceramic particles within the examined regions (Furong et al., 2022).

Although the selected processing condition reduced the visible inter-bead gaps, localized microscale voids were still observed in the printed green parts. These defects are inherent to the layer-by-layer deposition mechanism of FFF and can influence the structural integrity of ceramic-filled green parts prior to subsequent debinding and sintering processes (Zhao et al., 2021).

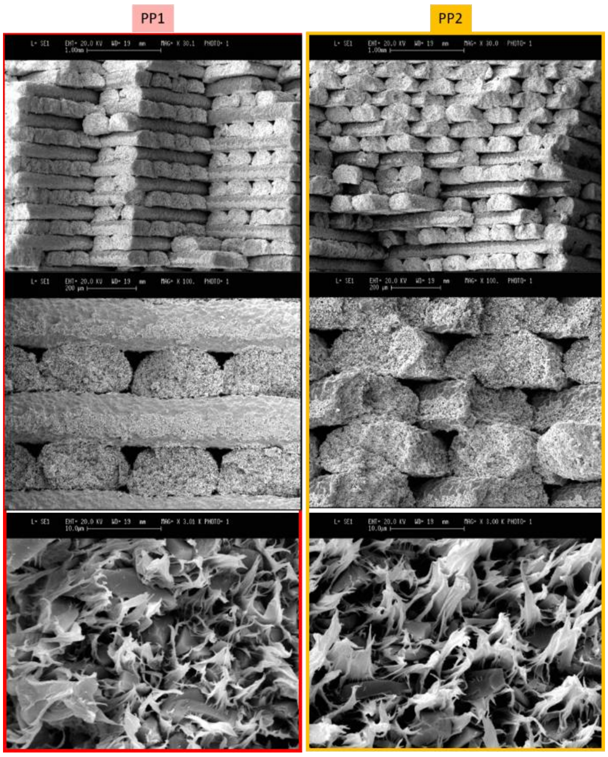

Figure 3. SEM micrographs of SiC/polymer green parts fabricated under different FFF processing conditions: PP1, fabricated using the selected printing condition (layer height: 0.4 mm, 100% linear infill, shell number: 1, nozzle temperature: 250 °C, bed temperature: 60 °C, printing speed: 15 mm s^{-1}, and flow rate: 110%), and PP2, fabricated under a comparative printing condition with a higher printing speed and lower nozzle temperature (layer height: 0.4 mm, 100% linear infill, nozzle temperature: 200 °C, bed temperature: 60 °C, and printing speed: 35 mm s^{-1})

3.4. Mechanical Properties of Printed Parts

The mechanical integrity of the FFF-printed SiC/polymer green parts was evaluated by three-point bending tests according to ASTM D790. The specimens were fabricated using the selected printing parameters and tested at a crosshead speed of 1 mm min^{-1}. The obtained flexural properties are summarized in Table 2.

The printed specimens exhibited an average flexural strength of 10.5 ± 2.5 MPa (with a mean fracture load of 33.9 ± 9.2 N), indicating adequate mechanical integrity and structural cohesion in the as-printed state. Considering that the green parts are mainly supported by the polymer binder phase before debinding and sintering, this level of strength indicates that the selected printing conditions provided adequate structural cohesion between deposited filaments. The observed standard deviation is attributed to the presence of localized printing-induced micro-defects, such as internal voids and variations in inter-bead contact. In particular, specimen No. 2 exhibited a lower fracture load (23.5 N) compared with the other samples (41 N and 37.2 N), which is associated with localized stress concentration sites. Overall, the obtained results indicate that the selected FFF processing conditions enabled the fabrication of mechanically stable SiC/polymer green parts suitable for subsequent processing. To further contextualize the significance of the findings, the flexural strength of the green parts obtained in this study (10.5 ± 2.5 MPa) was compared with values reported in similar extrusion-based additive manufacturing studies of ceramic/polymer systems.

Previous studies have demonstrated the importance of FFF processing conditions and defect control in the fabrication of SiC and other ceramic components. (Goulas et al., 2025). investigated material extrusion-based FFF of SiC and showed that appropriate processing and subsequent sintering can lead to near-full-density SiC components with high mechanical performance. Similarly, (Gauthe et al., 2025). demonstrated that process optimization and control of printing-related defects are important for achieving high-strength SiC components. (Orlovská et al., 2020) also reported that printing conditions, particularly layer thickness, influence the density and mechanical properties of FFF-processed alumina ceramics after sintering. Although these studies mainly evaluated the properties of the final ceramic components, their findings emphasize the importance of controlling the quality of the as-printed structure as a prerequisite for successful subsequent thermal processing. For comparison, in our previous study (Ghelich et al., 2026), a flexural strength of 1.08 ± 0.05 MPa was obtained for as-printed PE/SiC green parts containing 60 wt.% SiC. In that work, the composite filament was prepared by extrusion, whereas a commercially available PE/α-SiC filament was used in the present study. Therefore, differences in binder formulation, filament processing history, ceramic loading, and printing conditions may contribute to the different mechanical responses, and a direct quantitative comparison should be made with caution. Nevertheless, the results of both studies highlight the importance of feedstock characteristics and FFF processing conditions in determining the mechanical integrity of SiC/polymer green parts.

In the present study, the selected printing condition, consisting of a nozzle temperature of 250 °C, printing speed of 15 mm s^{-1}, and flow rate of 110%, resulted in improved filament contact and fewer visible inter-bead gaps compared with the comparative condition. The average flexural strength of 10.5 ± 2.5 MPa obtained under this condition is consistent with the improved inter-bead contact observed in the SEM micrographs. These results indicate that the selected processing condition provided adequate mechanical integrity in the as-printed state and establishes a useful baseline for subsequent debinding and sintering studies.

TABLE 2. Flexural properties of the FFF-printed SiC/polymer green parts

Sample	Width (mm)	Thickness (mm)	Fracture load (N)	Flexural strength (MPa)
1	10.29	4.84	41.0	12.7
2	9.96	4.76	23.5	7.8
3	9.95	5.01	37.2	11.1
Average ±SD	—	—	33.9±9.2	10.5±2.5

3.5. Demonstration of complex geometry fabrication

To further demonstrate the applicability of the selected printing parameters beyond standard test specimens, a complex-shaped SiC/polymer green part was fabricated using the optimized FFF processing conditions. As shown in Figure 4, the selected parameters enabled successful deposition of the ceramic-filled filament into a geometrically complex structure while maintaining the overall intended shape. The successful fabrication of this demonstrator indicates that the selected printing conditions provided sufficient process stability for producing geometrically complex SiC/polymer green parts prior to subsequent debinding and ceramic conversion processes.

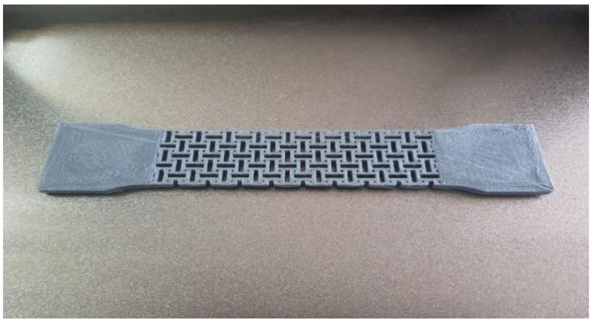

Figure 4. Complex-shaped SiC/polymer green part fabricated by FFF using the selected printing parameters, demonstrating the capability of the developed processing conditions for producing geometrically complex structures.

Overall, the results indicate that the selected FFF processing conditions enabled the fabrication of SiC/polymer green parts with adequate microstructural and mechanical integrity, providing a practical basis for subsequent debinding and sintering studies. The present study focused on the as-printed green state; therefore, the debinding and sintering behavior and the properties of the resulting SiC ceramics were not evaluated. In addition, localized microscale inter-bead voids remained despite optimization of the printing parameters. Further studies should investigate the complete debinding and sintering process and evaluate the resulting density and mechanical properties.

4. CONCLUSION(S)

This study demonstrated the feasibility of fabricating SiC/polymer composite green parts using fused filament fabrication by investigating the thermal behavior, microstructure, and mechanical performance of a commercial PE/α-SiC filament. Thermal analysis of the composite filament provided valuable information for defining a suitable processing range, indicating relatively limited mass loss below approximately 360 °C and a major binder degradation region between 360 and 474 °C. Microstructural evaluation of the raw filament showed a relatively uniform distribution of α-SiC particles within the polymer matrix without significant particle agglomeration. The internal structures of green parts fabricated under the selected and comparative printing conditions were evaluated through SEM analysis.

The selected printing condition resulted in improved deposition continuity and better inter-bead contact compared with the comparative printed specimen. Although localized microscale voids remained within the printed structures, the obtained green parts exhibited sufficient structural integrity for handling and subsequent ceramic conversion processes. The fabricated specimens showed an average flexural strength of 10.5 MPa, demonstrating the mechanical capability of the printed SiC/polymer green parts.

Furthermore, the successful fabrication of a complex-shaped component demonstrated the capability of the selected FFF processing conditions to produce geometrically complex SiC/polymer green parts using a commercial ceramic-filled filament.

ACKNOWLEDGEMENTS

This project was supported by the Center for International Scientific Studies and Collaboration (CISSC), under grant number 4040055, Ministry of Science, Research and Technology of Iran.

REFERENCES

1. Abdulhameed, O., Al-Ahmari, A., Ameen, W., & Mian, S. H. (2019). Additive manufacturing: Challenges, trends, and applications. Advances in Mechanical Engineering, 11(2), 1687814018822880. (https://doi.org/10.1177/1687814018822880)

2. Alfattni, R. (2022). Comprehensive study on materials used in different types of additive manufacturing and their applications. International Journal of Mathematical, Engineering and Management Sciences, 7(1), 92. (https://doi.org/10.33889/IJMEMS.2022.7.1.007)

3. Arnesano, A., Padmanabhan, S. K., Notarangelo, A., Montagna, F., & Licciulli, A. (2020). Fused deposition modeling shaping of glass infiltrated alumina for dental restoration. Ceramics International, 46(2), 2206–2212. (https://doi.org/10.1016/j.ceramint.2019.09.205)

4. Camargo, I. D., Fortulan, C. A., & Colorado, H. A. (2022). A review on the ceramic additive manufacturing technologies and availability of equipment and materials. Cerâmica, 68(387), 329–347. (https://doi.org/10.1590/0366-69132022683873331)

5. Deckers, J., Vleugels, J., & Kruth, J.-P. (2014). Additive manufacturing of ceramics: A review. Journal of Ceramic Science and Technology, 5, 245–260. (https://doi.org/10.4416/JCST2014-00032)

6. Fan, Z., Tan, Q., Kang, C., & Huang, H. (2024). Advances and challenges in direct additive manufacturing of dense ceramic oxides. International Journal of Extreme Manufacturing, 6, 052004. (https://doi.org/10.1088/2631-7990/ad5424)

7. Furong, N., Xiaole, Y., Yuanbing, L., Jinyu, G., Peng, L., Zhipeng, X., & Xianfeng, Y. (2022). Fused deposition modeling of Si_3N_4 ceramics: A cost-effective 3D-printing route for dense and high-performance non-oxide ceramic materials. Journal of the European Ceramic Society, 42(15), 7369–7376. (https://doi.org/10.1016/j.jeurceramsoc.2022.08.058)

8. Gauthe, M., Lorrette, C., Chaffron, L., Calme, S., Tonnellier, X., Rodolfo, J., & Sortais, Y. (2025). Fused filament fabrication of silicon carbide parts: A strategy for producing high-strength components. Journal of the European Ceramic Society, 45, 117229. (https://doi.org/10.1016/j.jeurceramsoc.2025.117229)

9. Georgopoulou, A., Sebastian, T., & Clemens, F. (2020). Thermoplastic elastomer composite filaments for strain sensing applications extruded with a fused deposition modelling 3D printer. Flexible and Printed Electronics, 5(3), 035002. (https://doi.org/10.1088/2058-8585/ab9a22)

10. Ghelich, R., Omidvar, H., Solgi, M., Razavi, M., & Neşer, G. (2026). Polyethylene–SiC composite filaments: Processing, printability, and formation of porous SiC preform via additive manufacturing. Journal of Materials Research and Technology, 42, 10612–10624. (https://doi.org/10.1016/j.jmrt.2026.05.060)

11. Gómez-Gómez, A., Moyano, J. J., Osendi, M. I., Belmonte, M., & Miranzo, P. (2021). The effect of rod orientation on the strength of highly porous filament printed 3D SiC ceramic architectures. Boletín de la Sociedad Española de Cerámica y Vidrio, 60(3), 119–127. (https://doi.org/10.1016/j.bsecv.2020.01.013)

12. Goulas, A., Ozkan, B., Ketharam, A., Saremi-Yarahmadi, S., & Vaidhyanathan, B. (2025). Additive manufacturing and characterisation of silicon carbide components fabricated using material extrusion-based fused filament fabrication. Ceramics International, 51, 50779–50786. (https://doi.org/10.1016/j.ceramint.2025.08.303)

13. Guo, H., Dafaalah, A. H., Liu, Y., Zhang, Y., & Qiu, G. (2020). A comparative study on the mechanical properties of polymeric monofilaments. Journal of Engineered Fibers and Fabrics, 15, 1558925020962790. (https://doi.org/10.1177/1558925020962790)

14. Jiménez, M., Romero, L., Domínguez, I. A., Espinosa, M. D. M., & Domínguez, M. (2019). Additive manufacturing technologies: An overview about 3D printing methods and future prospects. Complexity, 2019, 9656938. (https://doi.org/10.1155/2019/9656938)

15. Jose, S. A., Crosby, J., & Menezes, P. L. (2026). Additive manufacturing of ceramics and ceramic-based composites: Processing, properties, and engineering applications. Ceramics, 9, 43. (https://doi.org/10.3390/ceramics9050043)

16. Mansfield, B., Torres, S., Yu, T., & Wu, D. (2019). A review on additive manufacturing of ceramics. In Proceedings of the International Manufacturing Science and Engineering Conference (p. V001T001A001). American Society of Mechanical Engineers. (https://doi.org/10.1115/MSEC2019-2849)

17. Orlovská, M., Chlup, Z., Bača, Ľ., Janek, M., & Kitzmantel, M. (2020). Fracture and mechanical properties of lightweight alumina ceramics prepared by fused filament fabrication. Journal of the European Ceramic Society, 40(14), 4837–4843. (https://doi.org/10.1016/j.jeurceramsoc.2020.02.026)

18. Travitzky, N., Bonet, A., Dermeik, B., Fey, T., Filbert-Demut, I., Schlier, L., Schlordt, T., & Greil, P. (2014). Additive manufacturing of ceramic-based materials. Advanced Engineering Materials, 16(6), 729–754.(https://doi.org/10.1002/adem.201400097)

19. Vozarova, M., Neubauer, E., Bača, Ľ., Kitzmantel, M., Feranc, J., Trembošová, V., Peciar, P., Kritikos, M., Orlovská, M., & Janek, M. (2023). Preparation of fully dense boron carbide ceramics by fused filament fabrication (FFF). Journal of the European Ceramic Society, 43(4), 1751–1761. (https://doi.org/10.1016/j.jeurceramsoc.2022.12.018)

20. Wille, T., Hopf, A., Layher, M., Bliedtner, J., Kerber, A., & Bloß, L. (2024). Investigations on the processing of ceramic materials using fused filament fabrication. Open Ceramics, 19, 100649. (https://doi.org/10.1016/j.oceram.2024.100649)

21. Zhao, L., Wang, X., Xiong, H., Zhou, K., & Zhang, D. (2021). Optimized preceramic polymer for 3D structured ceramics via fused deposition modeling. Journal of the European Ceramic Society, 41(10), 5066–5074. (https://doi.org/10.1016/j.jeurceramsoc.2021.03.045)

22. Zocca, A., Colombo, P., Gomes, C. M., & Günster, J. (2015). Additive manufacturing of ceramics: Issues, potentialities, and opportunities. Journal of the American Ceramic Society, 98(7), 1983–2001. (https://doi.org/10.1111/jace.13700)